2. ACCELERATOR AUGMENTATION PROGRAM

2.1 LINAC

S. Ghosh, R. Mehta, G.K. Chowdhury, A. Rai, B.K. Sahu, A. Pandey, D.S. Mathuria, S.S.K. Sonti, K.K. Mistry, P. Patra, S. Ojha, A. Sarkar, R. Joshi, J. Zacharias, P.N. Prakash, A. Mandal, D. Kanjilal and A. Roy

2.1.1 Tests in Simple Test Cryostat

During last academic year, the usage of test cryostat was reduced as the LINAC cryostat related activity had been intensified. However, the test cryostat had been used a few times to perform cold tests to check the performance of a resonator and to check the performance of a modified slow tuner. The performance of the resonator was measured to be 3.0 MV/m at 4 watts of input power. In other cold test involving the modified slow tuner, the recurring leak problem of the indium seal was solved and the slow tuner was able to control the frequency drift (~ +/- 30 kHz) while locking the resonator frequency at some reasonable field level.

Besides this activity, test cryostat had been used for temperature mapping of the resonator at its various internal parts. This test was performed to understand the temperature difference between the outer stainless steel jacket and some of the interior places of the resonator e.g. at the tip of the drift tube. After attaining the thermal equilibrium, the temperature difference between the outer jacket and at the tip of the drift tube had been measured and found to be ~ 5 K while baking and 80 K while cooling down the resonator with LN_2. These set of data will be helpful to understand the temperature of different internal parts of the resonator during baking and cooling of the resonator by measuring the temperature on the outer Stainless Steel jacket of the resonator.

2.1.2 Activities related to LINAC and superbuncher (SB) cryostat

Offline and online tests of resonators in LINAC and SB cryostat

During last academic year, four cold tests with four to eight resonators in LINAC cryostat were performed. Same numbers of cold tests were also performed for the single resonator in buncher cryostat.

First test

During the first offline test, three resonators along with a superconducting solenoid [1] were installed in the LINAC cryostat. Once superconducting, all the three resonators in LINAC and the resonator in SB had come out from multipactoring barrier within 36

hours. The resonators in SB and LINAC cryostat had been resonating at the same frequency of 97.0 MHz. High power pulse conditioning for a short duration (~15 minutes) was done on LINAC resonators and the field achieved for two resonators were ~ 2.6 MV/m @ 5-6 watts of input power. The power cable of one LINAC resonator got damaged and consequently, it didn't perform well. As a matter of fact, the power cable of the all the LINAC resonators were not able to sustain a higher power and higher temperature (> 60^{o}C), so high power conditioning for a long duration could not be done. The performance of the superbuncher resonator was found satisfactory.

During the on-line beam test following the first off-line test, $^{28}Si^{+8}$ beam was prebunched and injected into the superbuncher. But the superbuncher could not be locked at 97 MHz as its drive coupler could not be moved all the way IN to achieve a reasonable beta (30-40) value. The two resonators in LINAC cryostat could be locked at 97 MHz with a reasonable field value. So two working resonators in the LINAC cryostat had accelerated the dc beam and splitting of the energy peak into two peaks separated by a valley was observed. By optimizing the reference phase difference between the two resonators, the maximum energy gain was found to be 2.6 MeV.

Second test

After this test, to increase the capability of the power cable to carry more power, eight LN_2 manifolds have been designed and installed inside the LINAC cryostat, so that most of the portion of the power cable would be immersed into LN_2. So when a power of ~ 300-400 watts would be flowing into the power cable, they would dissipate the heat in LN_2. The whole power cable system was tested with 300 watts of power for 48 hours and no damage to the cables was observed. The drive coupler problem of the SB was also solved and tested in cold condition before testing the SB with LHe.

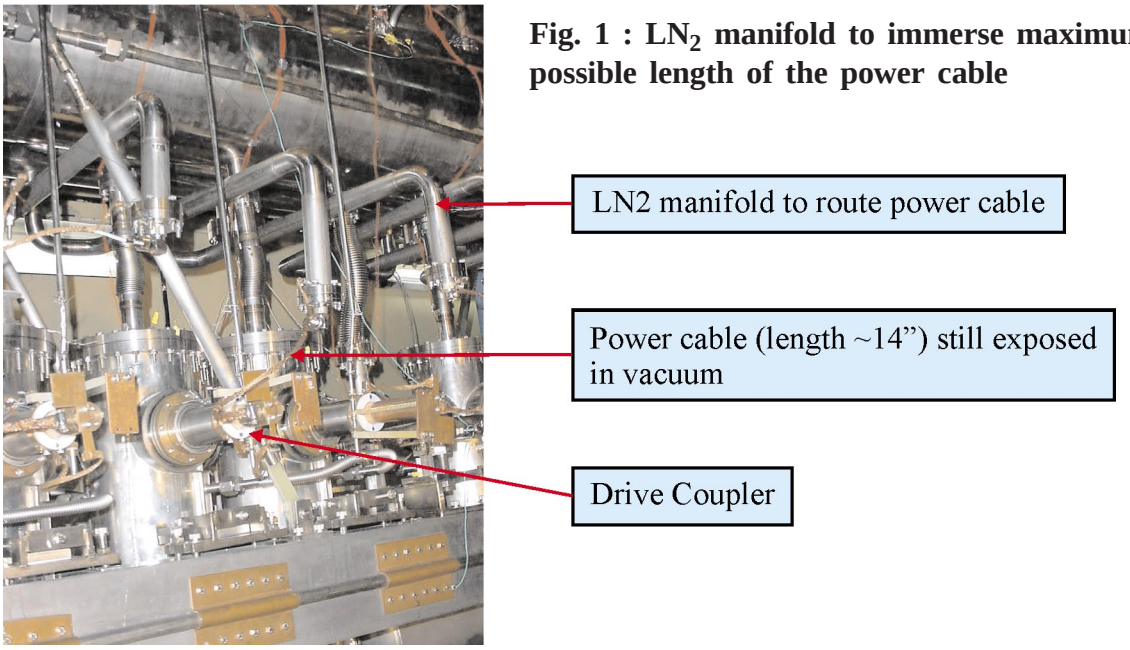

Fig. 1 : LN_2 manifold to immerse maximum possible length of the power cable

During the second off-line cold test of the resonators in LINAC cryostat, the same three resonators were used. The objective of this test was to check the reliability of the entire system under actual running condition. The same two resonators, which were used in first on-line beam test, had been locked by the master oscillator at 97.0 MHz at a field level of 4.3 and 3.1 MV/m with a forward power of 200 and 210 watts respectively for a period of 8 hours. The measured performance of the third resonator was found to be not so good (achieved accelerating field, Ea = 1.5 MV/m @ 5 watts of input power) and it could not be phase locked at a reasonable field. But unfortunately as the slow tuner line of the SB got choked, it could not be locked against the Master oscillator and the on-line beam test could not be completed.

Third test

Three resonators in LINAC cryostat and the single resonator in SB cryostat had been again tested to check reliability and repeatability of the good performance from the previous test. The field obtained from the first two resonators of the LINAC cryostat was 4.3 and 3.8 MV/m at 6 watts of input power, but the performance of the third resonator didn't improve. Due to prolonged baking of the resonators, indium seal of the slow tuner flanges of the resonators in LINAC cryostat had developed a leak in cold condition and the resonators could not be brought to the correct frequency.

After solving the leak problem all the eight resonators had been installed and aligned in to the LINAC cryostat #1 (Fig. 2.). All the power cables of the eight resonators were immersed in LN_2.

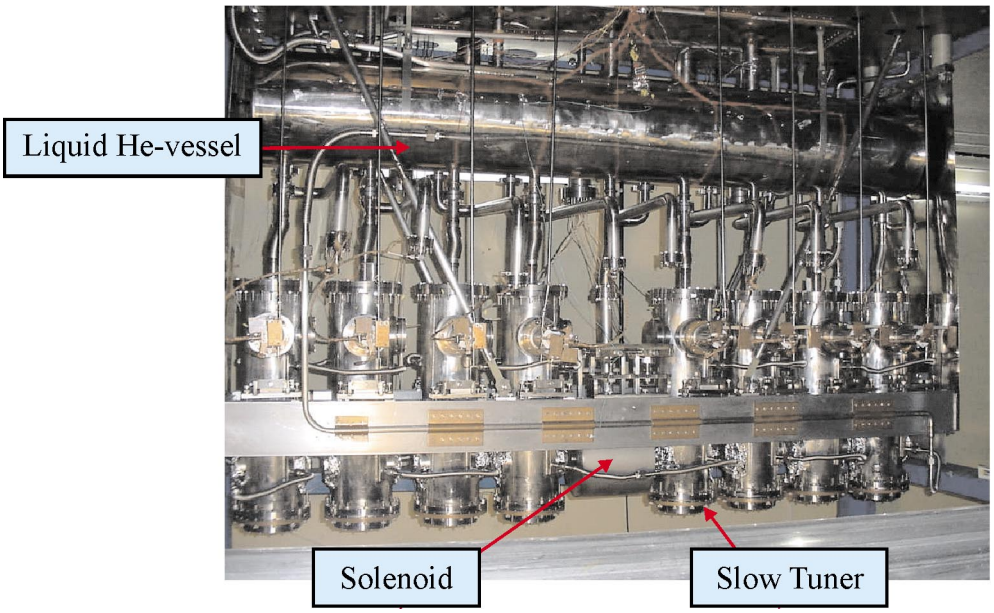

Fig. 2 : Eight resonators with a solenoid were installed in the first LINAC cryostat

Fourth test

During the fourth offline test seven out of eight resonators in LINAC cryostat were powered. Out of seven cavities, only four could be conditioned and phase locked. All the four resonators had maintained a stable lock at a field of 1.6 to 2.2 MV/m at an incident power of 170 to 240 watts.

Two of the resonators did not come out from multipactoring barrier and a cable fault in cold condition was suspected. The seventh resonator frequency was a few kHz off from the other resonators. However, after its slow tuner bellow was pressurised for a few days, its resonant frequency was brought close to the master oscillator frequency. But due to lack of time, this particular resonator could not conditioned at high RF power and the field level was low.

During the on-line beam test, the master oscillator resonating at 6.06 MHz along with the clock distribution module supplied the phase locked frequency to Multi Harmonic Buncher (MHB), High Energy Sweeper (HES), Phase detector (PD), single resonator in SB and five working resonators in LINAC cryostat. First the dc beam of $^{28}Si^{+7}$, 90 MeV was prebunched by MHB with post tandem HES removing the dark currents. A time width of 1.5 ns was injected into the resonator inside SB. The elastically scattered particles from a gold target were recorded in a fully depleted 40 μm surface barrier (SB) detector installed in a scattering chamber at the entrance of LINAC. The detector was cooled to –5^{o}C to reduce the noise and to improve time resolution. By properly adjusting the phase and amplitude of the resonator acting as the superbuncher, a FWHM of 360 ps of the time bunch was measured by the TAC at the entrance of LINAC. The intrinsic time width of the bunched beam after correcting for the detector resolution was estimated to be ~ 300 ps. The spectrum is shown in figure 3.

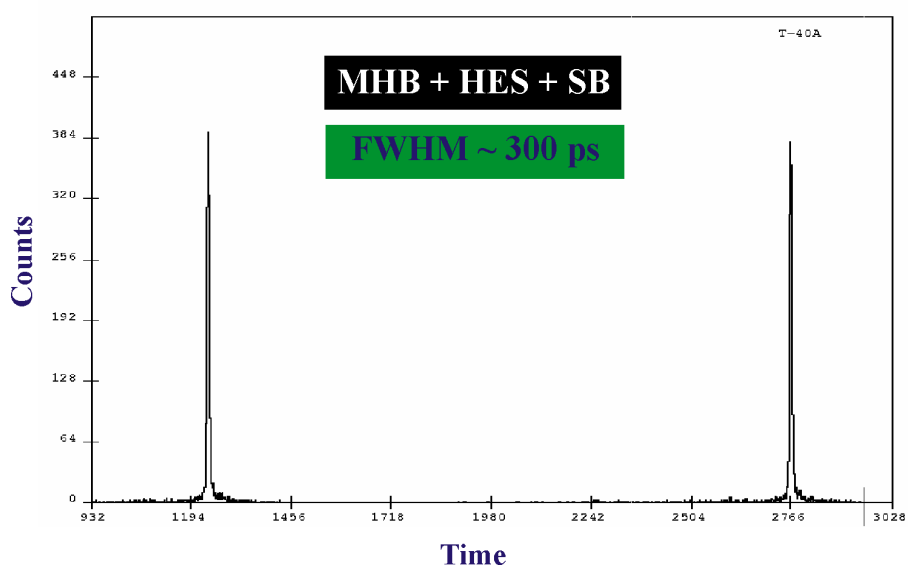

Fig. 3 : Time width of the beam bunch to be injected in to LINAC

The bunched beam of 300 ps was injected into the resonators of the LINAC cryostat. With the help of second set of SB detectors along with gold foils mounted in the second scattering chamber at the exit of LINAC, the energy centroid of the bunched beam from SB was measured while all the resonators were off. Then the first resonator was turned on and its phase was varied in such a way that the energy centroid of the beam coincided with the value of the centroid when all the resonators were off. Thus the zero cross over of the RF field of the first resonator was found out. The RF phase of this resonator was advanced by 70 degree or decreased by 110 degree depending upon the zero cross over point of bunching or de-bunching mode, to shift the energy centroid in the positive direction to confirm energy gain from this resonator. In this way, all the remaining four resonators were optimised to maximize the energy gain of the beam. The total energy gain measured at the exit of LINAC was close to 6 MeV [2] as shown in figure 4. No major problem was faced while accelerating the beam through five resonators of LINAC. The transmission of the beam through LINAC was close to 100%.

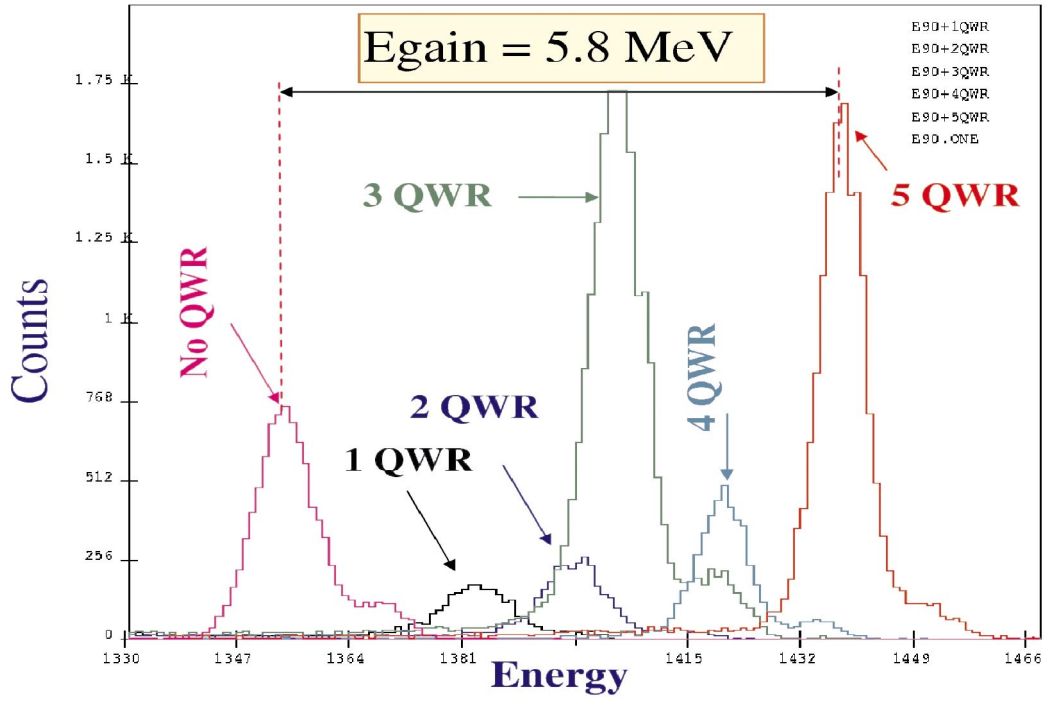

Fig.4. Energy gain of $^{28}Si^{+7}$ from five resonators of first module of LINAC

The accelerating field and hence the energy gain measured during this experiment was lower than the designed value. During various offline tests in the past, we had observed much better performance from the resonators. After opening the LINAC cryostat it was discovered that material from the drive coupler had evaporated and coated the inside of the resonator, resulting in high losses and the poor field levels. The resonators are being cleaned and efforts are on to improve the accelerating field of the resonators in LINAC cryostat.

REFERENCES:

[1] NSC Annual Report 2003-2004, page 10
[2] S. Ghosh et al., Indian Particle Accelerator Conference – March 01-05, 2005 at Kolkata, to be published

2.1.3 Indigenous Fabrication of Superconducting Niobium Resonators

P.N.Prakash, S.S.K.Sonti, J.Zacharias, K.K.Mistri

In the second stage of niobium resonator fabrication two completely indigenous resonators along with the slow tuner bellows have been built. Production of fifteen more resonators for the second and third LINAC modules will begin shortly.

2.1.3.1 Indigenous Fabrication of QWRs

After the successful completion of the first quarter wave resonator [1], construction of two more resonators in the second stage was taken up. This project was more challenging, since unlike the first resonator where extra parts from the Argonne project were used, these two resonators were fabricated completely indigenously. All machining, forming, rolling and fitting was done at a local vendor's site and the electron beam welding, electropolishing and heat treatment was done at NSC. Substantial amount of development work was undertaken to train the vendor manpower in machining, forming and handling niobium material. Simultaneously e-beam welding parameters of those welds that were not made during the fabrication of the first resonator, were also developed. Figure 1 shows one of the resonators along with its slow tuner bellows. Figure 2 shows a close up view of the slow tuner. Due to breakdown of the acid pumping system in the surface preparation lab the resonator could not be electropolished for cold tests. We expect to have the test results within the next several weeks.

2.1.3.2 Resonator Production

Towards the end of the fabrication of the two completely indigenous resonators, plans for producing fifteen more QWRs for the 2^{nd} and 3^{rd} LINAC modules started. Assessment of niobium material & contingency, explosion bonding of niobium to stainless steel, procurement of other materials, vacuum fittings, transition flange bellows etc. have started. Technical discussions with outside vendor, minor design changes, modification of drawings etc. are simultaneously being done. In order to increase productivity in electron beam welding and reduce the total welding time, a multi-spindle fixture with matching tailstock is being designed. The actual production work will start within the next one month.

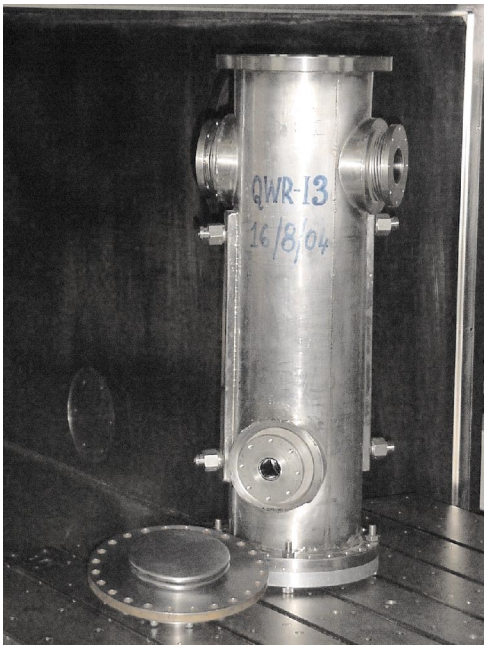

Fig 1: Completely indigenously built QWR along with the slow tuner bellows.

Fig 2: Close up view of the slow tuner.

REFERENCES

[1] NSC Annual Report 2003-04, p14

2.2 CRYOGENICS

T. S. Datta, Jacob Chacko, Anup Choudhury, Joby Antony, Manoj Kumar, Suresh Babu, S. A. Krishnan, Soumen Kar, R. S. Meena, R.G. Sharma and A. Roy

In this period, a total of seven helium cooling cycles have been performed for various offline and on line test including the first successful beam acceleration test during September 2004. During the beam acceleration test, the whole cryonetwork system has been kept at 4. 5 K for 15 days without any interruption, so far the longest run. A number of attempts were made to measure the total refrigeration load at 4.5 K from the partly established LINAC. Other than the routine operation and maintenance of cryogenic facilities, upgradation of storage capacity for liquid nitrogen and impure helium gas has been done in this period. An oil free helium gas compressor is added to the facility to save electrical power while recycling pure helium gas from offline test cryostat. Many new activities like development of superconducting quadrupole magnet, vortex tube refrigerator, liquid nitrogen driven prime mover have been initiated in this period. A number of experiments have been conducted to identify the source of fluctuation on temperature reading with RF.

2.2.1 Operation Experience on Cryo Network System

The cryogenic network system at Nuclear Science Centre, consisting of the helium and nitrogen refrigerator, cryogenic modules with the cavities and cryogen distribution lines, is now in routine operation for the preliminary testing of LINAC with and without beam. In total seven close loop mode cooling cycles have been performed in this period for in-beam and off-beam tests. Average duration of each run is 7 days with a maximum of 15 days during first successful acceleration test in September 2004. A few critical observations during cooling is reported here along with the action initiated to solve the minor problems encountered on cooling

a) Two phase flow on cooling liquid Nitrogen shield of LINAC cryostat

Intermediate thermal shield of LINAC module is cooled by forced flow of liquid nitrogen. In spite of adding one control valve with low Cv, it's difficult to maintain constant flow rate of 20 litres/hr. Either flow stops and which enhances the shield temperature or two phase flow in return line of nitrogen refrigerator disturbs the operating system. Frequent controlling of LN2 shield supply valve can be overcome by adding a phase separator in the return line of shield flow. Alternatively two immersion heaters in the buffer tank of LN2 vessel with control power feeding through liquid nitrogen level sensor are currently incorporated to have the single phase gas flow in the suction line of refrigerator.

b) Slow cool down rate of cavities in LINAC

In order to maintain a cool down rate (15-20 K/hr) of cavities in the critical zone between 140 K and 90 K a design to incorporate two parallel valves with bayonet connection and feeding the cold gas at 80 K point in the refrigerator has been completed. This will enhance the gas flow rate as well as cooling rate and lead to simpler operation with minimum human interference.

c) Cryostat Vacuum

On pre-cooling of cavities up to 150 K and with shield temperature at 100-120 K, achieved vacuum is better than 3×10^{-7} torr. Significant vacuum improvement was not noticed on cooling it down to 4.5 K and average ultimate vacuum is 8×10^{-8} torr, less than the expected value. Helium or nitrogen leak was not traced by residual gas analyzer and at the same time depletion of hydrogen ions was noticed which did not reflect in total pressure. Vacuum profile of LINAC module during cool down is shown in figure 1.

d) RF activity on temperature sensors

As reported earlier, temperature of shield, cavities and helium vessel is monitored by Lake Shore make DT470 silicon diode sensor. In the LINAC module, 16 sensors are

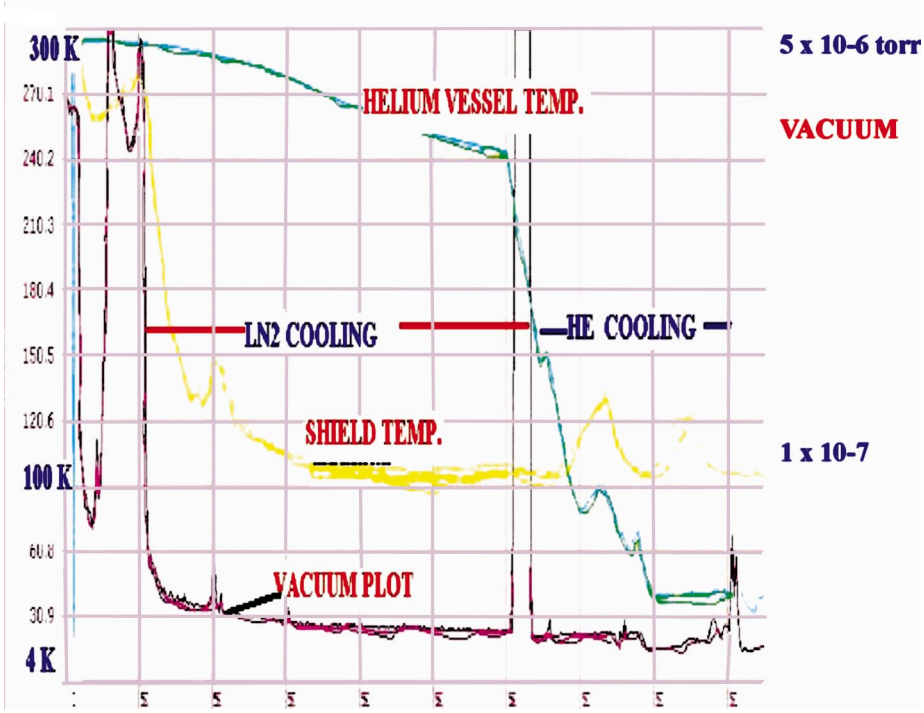

Fig 1 : Vacuum profile of LINAC module

divided into two OEN connectors and two indigenously developed meters with common current source. The temperature readouts were found to be fluctuating during RF powering of resonators in the cryostat and it was more prominent when resonators are out from multipactoring barrier. One such fluctuation is shown in figure 2.

The temperature readout fluctuation has been studied in detail and it appears that common grounding of sensor leads along with RF grounding through the cryostat body is the main source of error. Individual current source and amplifier are being provided for the temperature sensors and RF filtering in the processing electronics will be incorporated as a precautionary measure.

e) During steady state operation of LINAC, slow tuner is able to take care of minor fluctuation of helium gas pressure over cavity and refrigerator suction pressure.

2.2.2 Total Heat Load Measurement from the Established Cryogenic system

The refrigeration load at 4. 5 K from LINAC cryostat, buncher cryostat and part of distribution line by isolating the LINAC and simulating the same condition by an immersion heater in 1000 litres capacity master Dewar was measured in three runs and was found to be in the range of 90 - 110 W. This value is considerably higher than the calculated load of 60 W.

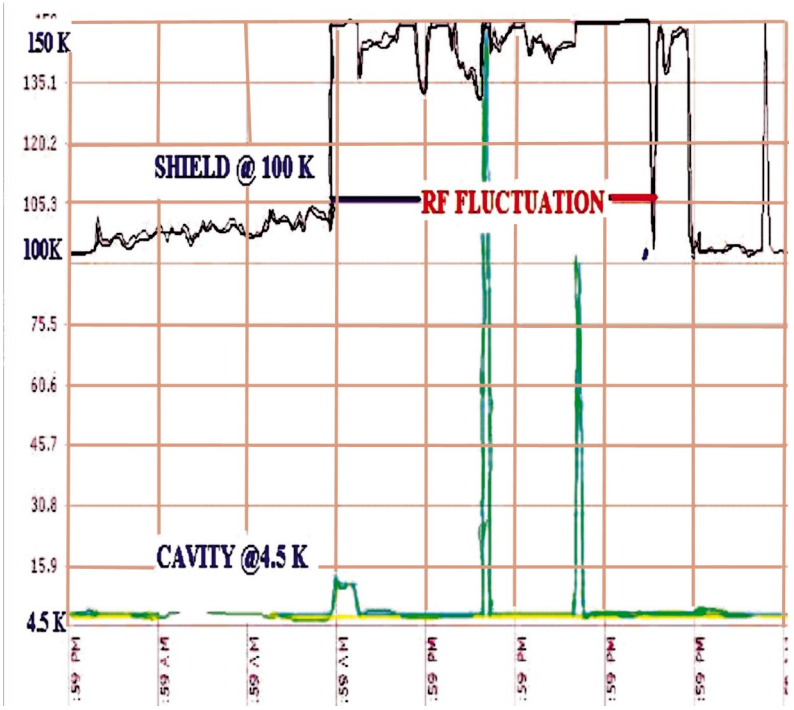

Fig. 2 : RF activity on temperature readings

As discussed earlier, the average static heat load for LINAC cryostat is about 8 W without cavities and RF related connections. From the present measurement on liquid level profile in LINAC cryostat with 8 cavities and RF connections, the average heat load is about 25 - 30 W. Similarly for buncher, it is about 7 W with all its accessories against its earlier value of 2.8 W. Liquid level profile in LINAC cryostat with and without cavities are shown in figure 3.

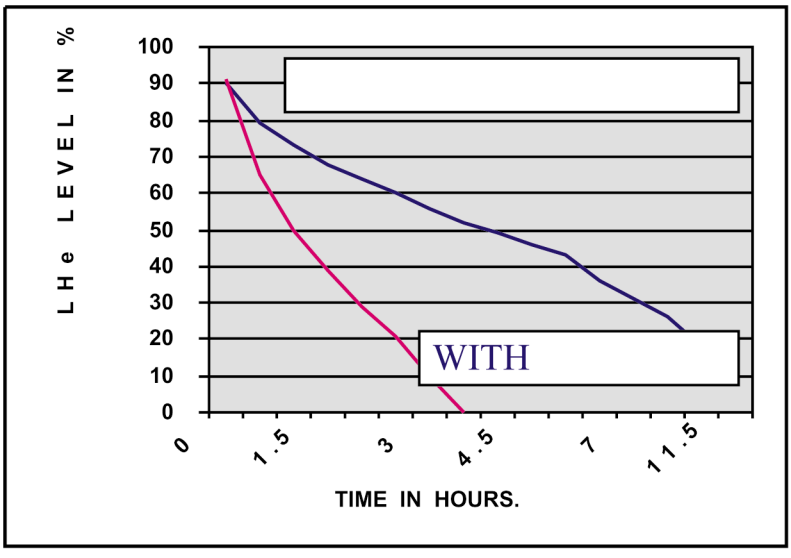

Fig. 3 : Liquid level profile in LINAC cryostat with & without cavities plus RF accessories

The average measured load on the small section of distribution line between LINAC and main valve box is about 30 - 38 W. This is significantly higher than the earlier measurement of 15 W (based on 1W/ meter). Higher shield temperature, poor vacuum in demountable section and thermal shorting are the possibilities for higher load. Also, the present liquid level meter has a minimum resolution of 20 litres which is equivalent to a heat load of +/– 60 W. Final analysis of breakup load value from the present measurement and comparison with predicted load is summarized in the following Table.

Table : Analysis of total heat load

Description	Expected load (Calculated) in W	Achieved Load (W)
LINAC Cryostat	15	25 - 30
Buncher	5	7 - 9
Distribution (LINAC part)	15	30 – 40
Distribution (Buncher)	25	25- 30
Total	**60 W**	**87 – 109 W**

Similarly, considering the total evaporation rate of 30 NM^3/hr from buncher and LINAC and total rise of temperature from 4.2 K to 13.5 K at the other end of distribution line, the calculated load is about 110 W.

2.2.3 Cryo Facility

2.2.3.1 Operation & Maintenance of Cryo Facility

Helium Plant: In this period plant was operated seven times mostly in refrigeration mode. The total production of liquid helium based on engine running hours (830) is about 90,000 litres. This is significantly higher than the previous two years. We had two major breakdowns due to malfunctioning of engine speed controller.

Nitrogen Plant: The plant was operated for 3050 hours and estimated liquid nitrogen production was 1,50,000 litres. Procurement from outside source was 1,60,000 litres. Routine maintenance on cryogenerator and compressor has been carried out.

Helium Recovery System: Complete overhauling of both the reciprocating compressors has been carried out by an external agency to solve the problem on high

interstage pressure and low capacity. Thirty purification runs on indigenously developed purifier have been performed to purify 3000 NM^3 impure helium gas.

2.2.3.2 Upgradation of facility

To have an uninterrupted supply of liquid nitrogen for a long LINAC run, additional storage vessel of 20,000 litres capacity is installed and commissioned. Measured evaporation rate for this container is 0.65% per day. Extra transfer line to integrate the present vessel with existing liquid nitrogen network is planned and designed. Commissioning of this line is expected by March 2005.

At present impure helium gas is stored in a cylinder manifold of 30 standard fifty liters capacity cylinders. In total there are about 100 joints which are prone to leak. To arrest this leak as well as to augment the storage capacity from existing 150 NM^3 to 300 NM^3, a high pressure (150 bar) horizontal storage tank has been designed, developed and installed at NSC. This cylinder is of 6 meters length and 0.75m diameter with wall thickness of 37 mm.

An oil free helium gas compressor with capacity of 30 NM^3/hr has been installed and commissioned to save electrical power on recycling the pure evaporated helium gas from offline test cryostat. Earlier same had been carried out by running main helium compressor with higher load (100 KW) compared to the present one of 6 KW to recover the helium gas at a rate of 10- 20 m^3/hr.

2.2.3.3 Activities related to electrical on Maintenance & Upgradation of cryogenic facility

Rajkumar

Remote Control Panel for Cold & Warm Helium Expanders

Cold and warm expanders are the main part of helium liquefier and their control panel is attached to liquefier body. The speed of the expanders is controlled through potentiometer and pressure transducer. A parallel system has been designed and developed to control and monitor the speed of expanders from the control room. This remote control panel has been interfaced with the local control using programmable logic controller (PLC). The speed control of the expander is being done through analog card of PLC's. Now we are able to operate & monitor the whole helium plant from the cryogenic control room.

Problems Encountered with FINCOR Controller & Alternate Method

Four quadrant FINCOR controllers are controlling helium expander brake motors.

During the recent runs we had multiple problems of fuse burning and follower cards going in saturation in these controllers. Finally problems were identified with the process control follower board. It was replaced with new one after tuning and calibration.

Alternatively, a new and low cost system is planned and tested for running the DC motor/generators. It actually converts pressure energy into electrical energy during the cooling process. We have devised a system for a controlled dissipation of this electrical energy into air by using heating elements. By controlling this energy, we are able to control the expander speed to desired level. We had one successful run of the plant using this system without use of FINCOR controller.

2.2.4 OTHER ACTIVITIES

2.2.4.1 Experiments with MLI

Earlier it was reported that the extraneous heat transfer on a nitrogen vessel surrounded by another nitrogen vessel was due to angular radiation from top plate at 300 K to the cylindrical surface at 77 through the annular gap. By reducing the gap with copper shield from 50 mm to almost zero, the heat load in 78K – 78 K configuration reduces from 1.48 W/m^2 to 0.3 W/m^2. In this period experiment has been conducted with copper shield for 78K – 4. 2 K configuration and the load is reduced from 0.8 W/m^2 to 0.24 W/m^2 for bare SS surface. Experiment was repeated with 5 layers of MLI and single layer of adhesive aluminium tape at various level of vacuum from 10^{-6} torr to 10^{-4} Torr.

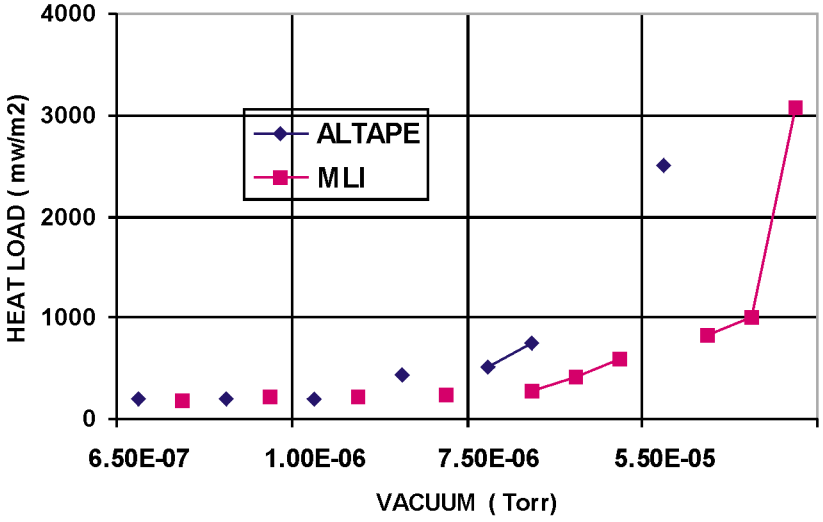

Fig. 4 : Heat load vs. vacuum

It is observed that at vacuum better than 10^{-5} torr, performance of single layer aluminium tape is comparable with 5 layers of MLI, otherwise MLI is better option than tape. Heat load data with Al tape and MLI against vacuum is shown in fig 4. To eliminate the angular radiation completely, a modification on existing set up is planned.

2.2.4.2 Vortex Tube

A device called Vortex tube is capable of producing low temperature up to –40°C from an input supply of air at pressure of 7 bar. This has been developed indigenously for study of various operating parameters related to the performance. Five such devices have been made with different dimensions and their performance is similar to commercially available tubes. Achieved minimum temperature is –40°C with no load.

Fig. 5 : Three Vortex Tubes

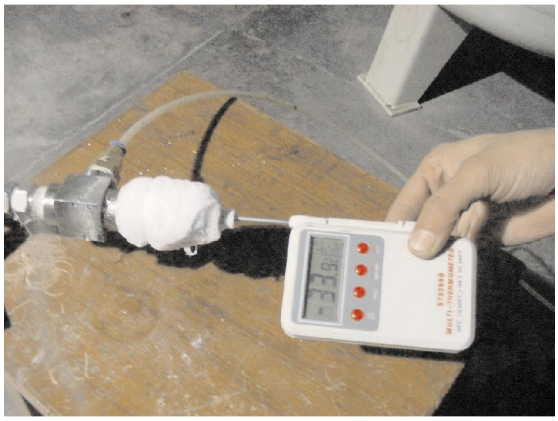

Fig. 6 : Cold tip measurement

These can be used for many applications where the spot cooling is required within this range of temperature from 0° C to - 40° C. Controlling the flow or the input pressure varies the refrigeration capacity and temperature. Nitrogen or helium gas would be used to see if the performance can be improved to achieve lower temperatures.

2.2.4.3 Development Of Superconducting Quadrupole Magnet

An wide bore (200 mm) cold iron superconducting quadrupole magnet for the HYRA project is under development. Based on the required input parameters from HIRA group, conceptual design of cryostat has been made. The critical features of this cryostat are high cold mass (1.8 Tons), low conductivity support structures, complex alignment mechanism and finally dimension restriction along the length. To meet the required dimension, the helium vessel, liquid nitrogen cooled shield and the vacuum jacket will be assembled in close tolerance with minimum gap. Aluminium tape rather than MLI on helium vessel is preferred considering space limitation. It has been decided to have all eight coils from Nb-Ti wire of approx. diameter 0.75 mm with formvar insulation and the operating current is 80 A.

2.2.4.4 Liquid Nitrogen Driven Motor

A heat engine that operates between atmospheric temperature as a heat source and cryogenic temperature as a heat sink is called a cryogenic heat (C-H) engine. A liquid nitrogen (LN2) powered heat engine is a best alternative zero emission engine concept compared to battery operated one. The development of this kind of engine has been initiated to study its possibility as a prime mover for lightweight applications. The preliminary stage of this project has been demonstrated by running a modified single cylinder, four-stroke engine as a two-stroke cycle expander based on open Rankine thermodynamic cycle.

Fig. 7 : LN2 driven prime mover

The idle speed of the engine for various injection pressure and mass flow rate has been measured. The load characteristics, mechanical and thermal efficiencies of the engine are yet to be measured. The exhaust gas temperature is less than ambient temperature and the engine efficiency increases with increase in atmospheric temperature.

2.2.5 Electronics Related Activities for Cryogenics and LINAC

Joby Antony and D.S. Mathuria

1. Design and fabrication of a 3 channel NSCISO double ended controller

This year, a new type thermometry controller has been designed and fabricated to study and analyse the RF related thermometry fluctuations. This has three independent channels with high precision independent current sources, no common ground between sensors, total isolation between channels, twisted pair inputs and outputs and RF rejection 30 dB down @97 MHz (measured). This was installed in LINAC1 using isolated 3

sensors to study the RF problem and found to be very effective in reducing the RF effects on LINAC thermometry.

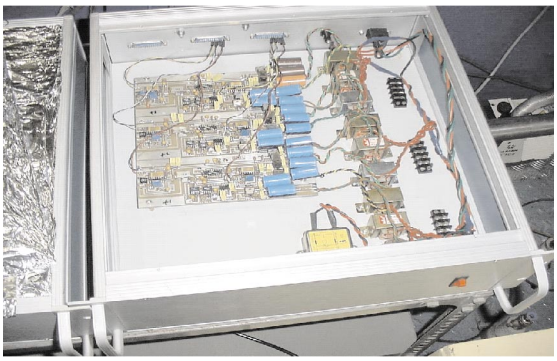

Fig. 8 : NSCISO inside view

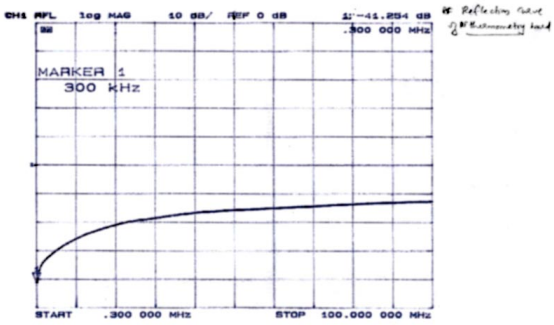

Fig. 9 : RF reflection curve of NSC ISO

2. Design and fabrication of a modified type 16 channel single ended thermometry controller (NSC620)

Two more single ended thermometry controllers of 16 channel each have been developed in this year. The earlier design is modified by using AD620 chips.

3. Set-up & experiments on RF effects of LINAC thermometry using new controller

On-line studies have been conducted by using NSCISO controllers and with three additional sensors attached to LINAC to identify the RF problem related to diode sensors when cavities were powered for the last LINAC experiments. Additional 3 sensors were installed separately in isolation with cryostat body The conclusion is that new type of controllers with isolated twisted pair inputs to differential ADCs along with shielded sensors could considerably reduce these effects on the thermometry.

Fig. 10 : Comparison of sensor reading

4. RF simulation studies using RF loop to study RF effect using Survey meter

A simulated test bench setup has been made to study the RF effects on P-N junction diode, which is being used for low temperature thermometry. DC voltage shift across the sensor has been observed with RF. And the shift is found to be proportional to the input RF power as shown below.

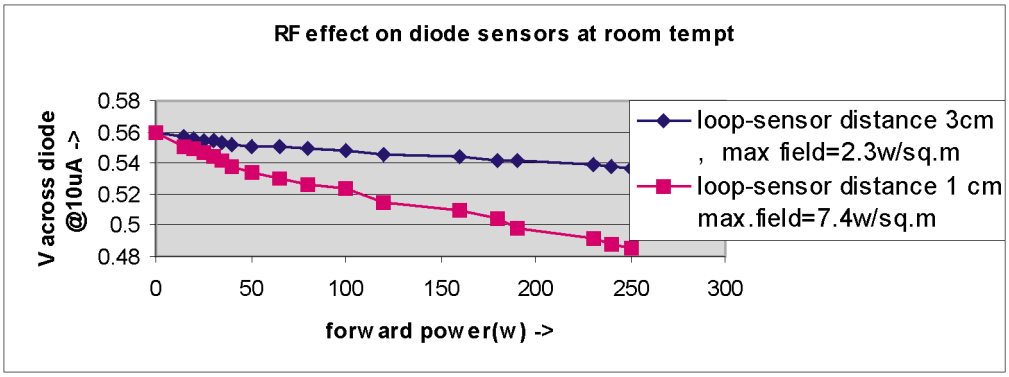

Fig. 11

5. Upgradation of CRYO-DACS to include a VME based heater control

A closed loop VME control of heater has been included to the present control system. The level read by level meter provides 4-20mA output and is compared with a virtual LLT and ULT settings provided by PC GUI. A digital output controls a relay in hysterics loop to power the heater, which in turn brings down the level. This system works independent of the PC, as program stays embedded.

6. EBW control system

The CRT touch screens of EBW machine has been replaced by LCD touch screens. The life of CRT touch screens is two to three years which is already over. LCD touch screen is having advantages like better quality picture; good for eye as it is flicker free, less power consumption etc. The gun light of EBW stopped working this year. The faulty analog board has been identified and replaced on priority basis. The system is back to normal.

7. SPL automation system

The indigenously developed LINUX based SPL automation has been commissioned in this year. Several minor problems are encountered and have been solved. Some modifications are incorporated as requested by users. It is developed on C++ with Qt interface.

2.3 RF ELECTRONICS

B.K.Sahu, Kundan Singh, Ashutosh Pandey, S.Venkataramanan, A.Sarkar and B.P. Ajithkumar

2.3.1 Computer Control System for Tandem-LINAC Accelerator

The control system work was completed and tested by taking beam through one LINAC module. The CAMAC Crate controllers were redesigned to have built-in disk-less single board computers. They load the operating system from a central server and run a server program to take care of the hardware devices connected to each Crate. The operator consoles are normal PCs with X-Window GUI and a shaft encoder interfaced to the parallel port acting as an assignable control knob.

The system is scalable to any number of servers/console clients. The system is totally based on open hardware standards and developed using Free Software tools. It supports multiple client programs to support partial automation of beam tuning. At present we are running eight CAMAC Crates and three consoles and more can be added without any change in software. Pelletron has been running on it for several years and one LINAC module has been tested this year. The following CAMAC modules were designed, fabricated for the control system.

a.	Intelligent CAMAC Crate Controller running Linux	15 nos.
b.	12 bit 16 channel DAC	2
c.	CAMAC interface for LINAC resonator controller	24
d.	Input Gate module	20
e.	Output register module	20
f.	Parallel port based shaft encoder circuits	3

2.3.2 Resonator control module

The aim of the resonator control unit is to adjust and maintain the amplitude and phase of the resonator constant with respect to the master reference. The approach for control is planned based on the principle of dynamic phase control. The circuit is designed in collaboration with Electronics division, BARC, Mumbai which is similar to the one being used for TIFR lead plated super-conducting cavities. The control module is tested thoroughly with 97 MHz superconducting cavities in a test cryostat and later with Super buncher cryostat. It is found that the control module can stabilize the phase of the super

conducting resonator up to 0.5 degree accuracy and amplitude with accuracy of 1%. Slow-tuner is basically used to bring the frequency of the resonator close to the master frequency and stabilize it there. In order to incorporate the slow-tuner with the fast control a interface circuit is designed and implemented with the resonator control circuit. Depending on the frequency error, slow-tuner control electronics work to bring the frequency close to reference by adjusting the pressure in the bellow and then during phase lock condition the phase error signal is used to take care of the slow scale perturbations to the resonator. Ten such modules were produced at Electronics Division, BARC and installed at NSC for the control of resonators housed in first LINAC cryostat in two special NIM bins with required power supply.

In order to operate the resonator control modules from remote, a CAMAC module is developed. The module contains 4 ADC, 4 DAC and 4 Output register and 4 input gate channels for control of a single resonator. The module also has additional interface for status and control of RF amplifiers. The database and page entry for this module is made in the same way as for other CAMAC modules used for pelletron operation. This module simplifies the interface work in comparison to interfacing the control by using standard CAMAC modules with a switchyard.

2.3.3 Development of 400 Watt, 97 MHz RF Amplifier

During the testing of the resonator with the resonator control it is realized that 200Watt RF amplifier used for the control may not be sufficient to stabilize the amplitude and phase of the resonator at higher field gradients. Since some of our resonators are capable of giving higher fields a 400Watt, 97 MHz RF amplifier is designed and tested. RF circulator and load is used at the output to take care of the reflected power. The amplifier is mounted on a specially made water cooled ETP copper heat sink. The technology is transferred to BEL, Bangalore for production of ten numbers of amplifiers as per initial requirements. A parallel production job is taken up at NSC for more numbers.

2.3.4 Slow-tuner mechanical assembly for LINAC

The slow-tuner mechanical assembly mainly consists of vacuum port, gas in-flow port and small volume manifold containing a voltage controlled proportional valve, a solenoid valve, pressure transducer and in-line helium filters. This manifold is later connected externally to the slow-tuner bellow. The assembly is housed in a leak proof pressurized vessel. The flow rates to the manifold from the valves are adjusted properly to work in synchronization of electronics control and decide the response time. After development it is tested with control electronics to stabilize the pressure in a given volume. Ten numbers of such channels were assembled in 3 different vessels and are being used with LINAC resonators.

2.3.5 Clock distribution system for LINAC

The clock distribution system is designed and developed to provide the master reference to the LINAC and its subsystems which include a multi harmonic buncher, high energy sweeper and phase detector. The circuit uses 6.0625 MHz as the fundamental frequency generated using a crystal oscillator specially made at BEL, Bangalore and generates the subsequent frequencies. The amplitude of all the frequencies is kept at 0 dBm. This is now being used with the LINAC control.

2.3.6 Status Report of the Multi-harmonic Buncher & the High Energy Sweeper and associated jobs

The multi-harmonic buncher (MHB) along with the high energy sweeper (HES) was operated to provide ^{16}O pulsed beam to the LINAC beam line for the acceleration of the beam through the LINAC. The FWHM of the beam was ~ 1.3 ns for short duration measurements. The phase of the beam was locked for long duration. The high RF voltage applied to the sweeper plates along with tightly closed sweeper slits could enable us to cut down the dark current between the pulses considerably. For the first time this pulsed beam was successfully accelerated through the LINAC. Since the LINAC cavities locked at 97.010 MHz instead of 97.000 MHz, the clock distribution module had to be changed during this run.

Apart from this, the multi-harmonic buncher was also operated along with the low energy chopper (of the old beam pulsing system) to provide a wide variety of pulsed beams to several users. Notable among them are the users of Saha Institute of Nuclear Physics (Kolkata), Punjab University, Delhi University, etc. The Traveling Wave Deflector was also used along with this integrated pulsing system on some occasions.

As a part of the duplication of the multi-harmonic buncher electronics, 12MHz harmonic generator module, distribution module etc. have been fabricated and tested in the laboratory. The fabrication of the other modules is in progress. Some spares for these modules have been ordered. A closed loop de-ionised water system has been installed in the vault area in order to provide proper water cooling to the sweeper coil.

Since the sweeper slits were installed (in the vault area) before the 48 MHz phase detector cavity (used for phase locking the MHB with beam) it used to be quite difficult to adjust the sweeper phase with tight slits in the phase locked condition of the MHB. A feasibility study was done to interchange the positions of the sweeper slits and the cavity phase detector in the beam line. Recently this work has been completed during the Pelletron maintenance.

2.4 BEAM TRANSPORT SYSTEM

A. Mandal, Rajesh Kumar and S.K. Suman

This laboratory takes care of regular maintenance, design and development of beam Transport System of the Accelerators in the centre. Several magnets and power supplies for the magnets have been designed and developed. Besides, this laboratory has ventured into developing high voltage power supplies for solid state detectors and electrostatic beam line components.

2.4.1 Design, Hardware fabrication and testing of a large acceptance Combined Function Analysing Magnet for PKDELIS ECR source

A. Mandal[1], G. Rodrigues[1], Peter Brodt[2], Frank Bodker[2] and D. Kanjilal[1]

[1] Nuclear Science Centre, New Delhi
[2] Danfysik, Denmark

A High Current Injector (HCI) which will inject multiply charged ions into the Superconducting LINAC is being built at Nuclear Science Centre. As a part of the HCI an ECR ion-source has been developed in collaboration with PANTECHNIK, France to deliver high current (a few pμA) heavy ion beams for LINAC . It is capable of operating at 14.5 GHz and 18 GHz using high Tc superconducting coils for axial fields. Due to the large axial magnetic field (~ 1.5 T), the emittance of the beam (being entirely dominated by this field) coming from the source is very large (~ a few hundred π mm-mrad) which poses a challenge in the design of Low Energy Beam Transport System (LEBT) to take account of space charge forces present in the multi charged beam extracted from ECR. The highly charged ions from ECR are first extracted at 30 kV and further accelerated using deck voltage, with a maximum allowable voltage of 350 kV. To reduce the loading of the high voltage power supply and space charge forces due to large multi-charged ions from ECR, a large acceptance analysing magnet is placed on the high voltage deck to pre-select ions of a particular charge state from the ECR source. The main design goals for the analysing magnet are large acceptance, minimum weight and reasonable mass resolution.

The High Current Injector will consist of a high performance High Temperature Superconducting ECR ion source PKDELIS followed by a Radio Frequency Quadrupole (RFQ) and Drift Tube LINAC (DTL). A new beam hall is being constructed on the east side of the present beam hall I to house these facilities. The schematic layout of the building and tentative layout of beam line is shown in figure-1.

Design of Analysing Magnet :

The magnet has been designed with the following beam parameters :

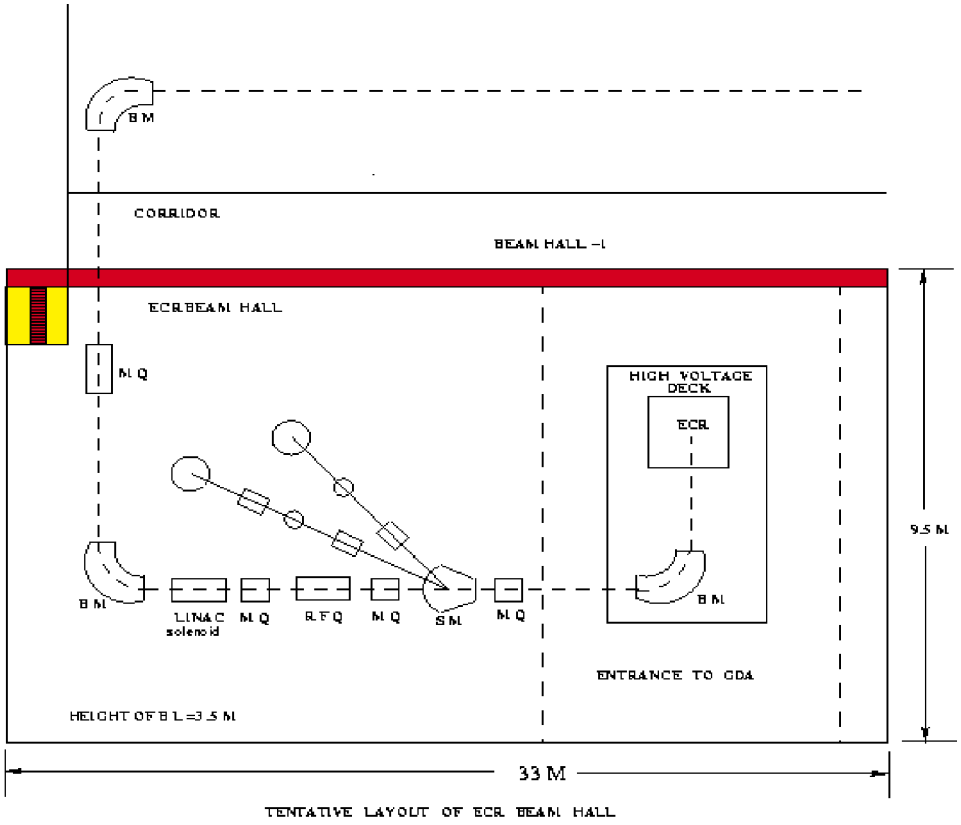

Fig. 1 : Layout of High Current Injector Beam Hall

Beam parameters:

ME/q2	=	0.3 a.m.u MeV
Magnet rigidity (Br)	=	0.09 T.m
Emittance	=	200 π mm.mrad

The analysing magnet is to be placed on a high voltage platform to reduce beam loading on high voltage deck power supply. Therefore the design aim is to have an air cooled, minimum weight, large acceptance, reasonable mass resolution magnet. The radius of the magnet which was chosen to be 0.3 m was optimised to minimise the weight. This gives a maximum field needed to be 0.3 T for ME/q2 = 0.3 a.m.u MeV considering a 90^o bend. The gap between two poles were optimised for different slit sizes so that good resolution is achieved without appreciable loss of beam and the weight is not too large. The following examples justify the selection of gap. For a slit size of 10 mm, y=5 mm, y' = 40 mrad, the beam size at the entrance turns out to be 24 mm and the mass resolution for 90^o magnet, $\Delta m/m = 1.7 \times 10^{-2}$. By taking smaller slit size the resolution can be improved at the cost of beam intensity. Otherwise the pole gap has to be increased resulting in increase of the weight of the magnet. The optimum gap of the magnet was found to be 80 mm for moderate resolution and minimum loss of beam intensity. This

resolution is good enough for mass region ~ 100 a.m.u, however, for higher masses it may be poor. Vertical focussing is obtained in a dipole magnet due to fringing field at the entrance and exit with particular entrance and exit angle. For a 90^o homogenous bending magnet double focussing is normally achieved with $\varepsilon_1 = \varepsilon_2 = 26.6^o$ and u = v = 2ρ. The above mentioned values of entrance and exit angle give double focussing if the gap of the magnet is small compared to the length of the magnet, However, because of large gap for this magnet we need larger entrance and exit angles. We have optimised entrance and exit angles for gap effect using TRANSPORT , GIOS and COSY INFINITY codes. The optimised value: $\varepsilon_1 = \varepsilon_2 = 32.8^o$ for u = v = 0.80 meter (instead of 0.6 m). In general the image suffers from aberration due to higher order terms, particularly for marginal beams. The most important contribution comes due to term containing x^2, y^2, x'^2, y'^2, xx', yy'. We have tried to minimise the geometrical aberrations due to higher order terms by incorporating multipole field components in the magnet itself. The vertical focussing is obtained by incorporating increasing sextupole field components at the entrance and exit. This is achieved by having cylindrical pole shape at entrance and exit with negative radius of curvature (0.24 m). The horizontal focussing is achieved by introducing decreasing sextupole field component in the radial plane at the middle of the magnet. The magnetic field in the x-plane (radial plane) can be expressed as

$$B = B_0 (1 + n_1(x / \rho) + n_2 (x / \rho)^2 + n_3 (x / \rho)^3 + ...)$$

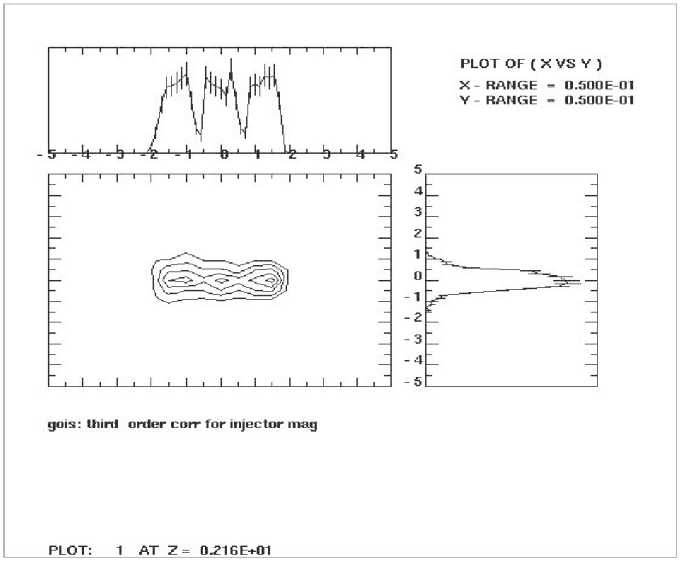

Fig. 2 : 3rd order Beam optics simulation using GIOS

where B_0 is the field at the centre. For a homogeneous magnet $n_1 = 0$. We have minimised aberations upto third order by varying n_2 and n_3 using GIOS and TRANSPORT code. The optimised values of the parameters are : $n_1 = 0$, $n_2 = -0.70$, $n_3 = 0.90$. To check the resolution we have introduced 1.5% mass dispersion. This is shown in figure 2.

As beam current is very high in ECR we have also considered the effect of space charge in the calculations. We find that the beam blows up significantly for a beam current of 1mA and a small fraction (~ 10%) of beam is lost pertaining to a gap of 80 mm. The order for fabrication of the magnet based on our design was placed to DANFYSIK, Denmark. The shape of the pole to match the specifications was designed using 3-D Vector field simulation program OPERA in collaboration with Danfysik engineers. After a lot of iterations the design was finalised to get the design goal.

The magnet was tested in Danfysik factory. The field was mapped using 3-D position scanner system and the average test results are summarised.

Parameters	NSC specifications	Model calculation	Measured value	Field (T)
Shim Angle (degree)	32.8±0.5	32	31.7±0.34	0.3
EFB-radius (mm)	240±10	250	255±20	0.3
n_1	0	0	0	0.3
n_2	-0.7±0.07	-0.694±0.001	-0.67±0.07	0.3
n_3	0.9±0.09	0.873±0.004	0.81±0.15	0..3
n_4	0	-0.032±0.046	-0.41±2.49	0.3

Thus we see that the different parameters of the magnet fabricated matches with our specifications within experimental errors.

2.4.2 Beam optics design of Low Energy Beam Transport System for ECR

A. Mandal and G. Rodrigues

Though ideally the designed double focussing magnet will focus beam if u=v=0.84m, however, in reality because of slight difference in measured parameters from design values. The beam will be distorted specially due to difference in the shim angle. Moreover, to accommodate extraction system and pumping unit actual distance between object point and magnet becomes more than 0.84 m. To have some play in image distance we have planned to introduce a quadrupole doublet between ECR and magnet. From beam optics simulation (fig.3) we find a short quadrupole doublet magnet helps in focussing as well as slight variation in the image distance.

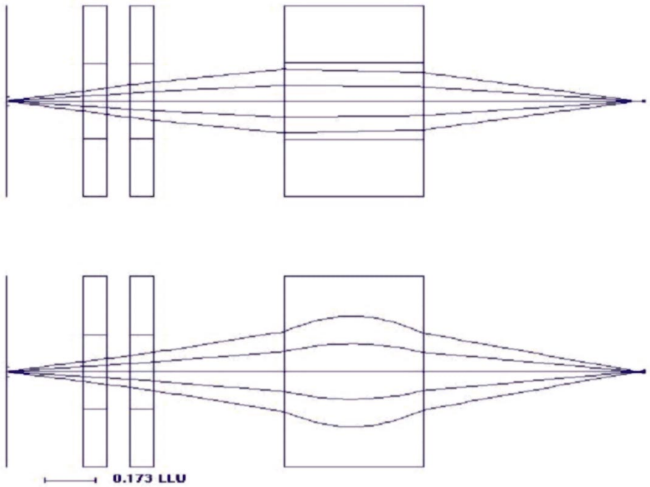

Fig. 3 : Beam optics simulation of LEBT of ECR

2.4.3 Design of a large area scanner

A. Mandal and P.L. Meena

A magnetic scanner has been designed for homogenous irradiation of large area of targets for materials science beam line in BH-II. The scanner has a capability of scanning beam over an area of 25x25 mm^2 for beam of 400 a.m.u MeV at a distance of 3metre at a frequency 50 Hz. The scanner consists of two H-shaped dipole magnets made of laminated silicon cores to minimise hysteresis loss. The magnets are placed perpendicular to each other. Schematic design of one magnet is shown in fig-4. The coils are air cooled.

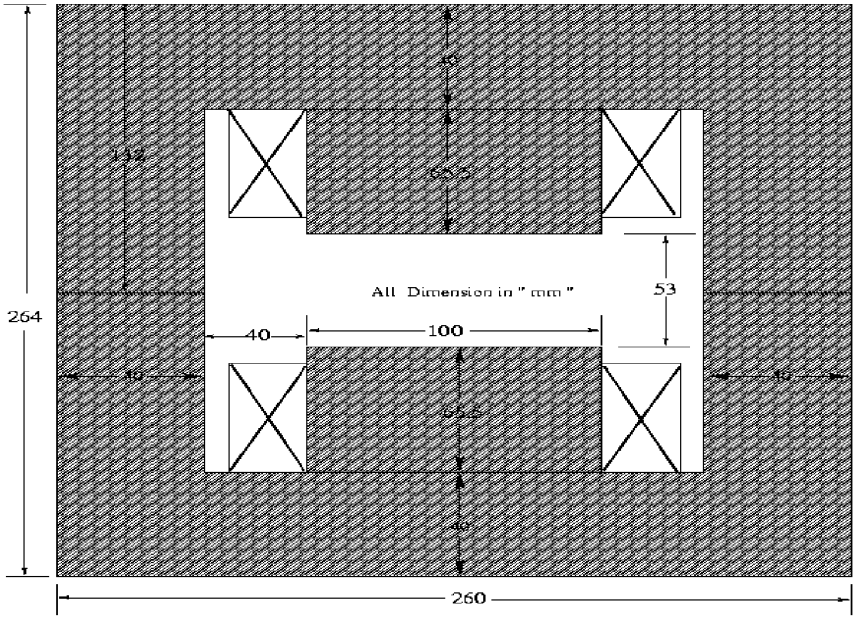

Fig. 4 : Schematic design of Scanner Magnet

The specifications of the magnets are as follows:

Shape H

Pole gap = 53mm

Maximum field = 1200 Gauss

Number of turns per coil = 48

Inductance for two coils = ~ 4mH

One coil has been made and tested for heat dissipation. The coil can withstand 40 Amp DC with a temperature rise of 35^0C.

2.4.4 Design of an Air cooled Quadrupole Magnet

A. Mandal and P.L.Meena

An air cooled magnetic quadrupole lens has been designed for focussing beam from RFQ in HCI beam line. Specifications are as follows:

Max. field gradient g	=	6.8 T/m
aperture radius	=	39 mm
pole tip field	=	0.26T
effective length	=	156 mm
Power for single Quad	=	140 W
Power supply (2 Quad)	=	15V,20A

One coil has been fabricated and tested for heat dissipation.

2.4.5 Beam Hall Activities

P. Barua, A. Kothari, M. Archunan, S.K. Suman and A. Mandal

Different activities in beam hall-II are summarised.

a) *Beam line installation* - reference for each beam line has been marked on floor as well as on wall with theodolite. All the quadrupoles have been installed and aligned. Two beam lines viz. Materials Science and Atomic Physics have been installed.

b) *Beam Hall shielding* - The radiation shielding as per plan has been carried out.

c) *Cable tray layout* - The trays for cabling to Data room and control room has been mounted.

d) *Water line* - The piping for cooling water is laid as per plan.

e) *Modifications in zero degree beam line* - Since some indigenously developed Faraday cup was not giving accurate beam current we have replaced them by NEC Faraday cup in zero degree beam line and replaced some defective beam pipes to improve vacuum in beam line.

f) *Modifications in vault I* - The phase detector was placed earlier after the slit which was causing problem in the phase lock of the pulsed beam during sweeper operation. This has been placed before the image slit of the analyser magnet.

g) *Installation of magnet power supplies and supporting BTS instruments* - All the power supplies were installed and connected to the respective magnets for local as well as remote operation and tested.

2.4.6 Fabrication of steerer Magnets

A. Mandal, S.K. Saini, Sunder Rao, S.K. Suman and Rajesh Kumar

Ten number of steerer magnets of three different designs have been fabricated for beam lines. The coils for these magnets were wound and assembled.

2.4.7 Development of a High Power Amplifier for Scanner magnet

Rajesh Kumar, S.K.Suman and A.Mandal

Beam Scanning magnets are used to scan ion beams on targets in x and y plane. The power supplies for these are AC amplifiers which can provide current regulated triangular wave. A prototype current regulated high power AC amplifier has been developed and tested. Amplifier has the following specifications.

- Triangular wave current output : 0 to ±50A
- Output Voltage Range : 0 to ±70V
- Scanning Frequency range : 0 to 50Hz depending on inductive load
- True current regulated output without cross over distortion
- Back emf protection
- Foldback type limits for over current and over voltage protection.

2.4.8 High Current High Stability Power Supply (300A/100V, 10 ppm)

Rajesh Kumar, Raj Kumar, Bishamber Kumar and A. Mandal

A 300A/100V, 10ppm linear current regulated power supply has been designed and developed for HYRA magnets. The prototype power supply has been assembled and tested. Specifications and performance results are given below.

Specifications :

- Stability class : ±10ppm/ 8hrs.
- Power range : 30kW
- Current range : 300A
- Voltage range : 100V

Performance :

- Drift and regulation data are given for maximum current output
- Drift (long term 8 hrs) : ±10ppm
- Line regulation (±10% change in line voltage) : ±1ppm
- Output ripple : 20mVpp
- Current setting : 16 bit (4.5mA)

For testing of power supply a 0.3R/30kW resistive load made of nicrom wire has been used.

2.4.9 Programable NIM based 5kV/100ìA Ge detector bias Power Supply

Rajesh Kumar, S.K.Suman, S.Muralithar and A.Mandal

A programmable 5kV detector bias supply for germanium and silicon detectors has been developed. It can be used with any detector that draws current less then 100uA and whose gain is insensitive to the applied voltage. The output can be ramped up and down at a programmable ramp rate.

Specifications:

- Output Voltage range : 0 - 5kV
- Rated output current : 0 - 100uA
- Output stability : < 0.1%
- Noise and ripple : < 10mVpp.

Features:

- Output voltage always starts from zero irrespective of the front panel setting.
- Output latches in case of power failure.
- Ready signal, when output achieved.
- Output can be ramped Up and Down.
- Output can be paused while ramping.
- Foldback type over current protection.
- Polarity reversal by changing daughter board position.
- 0- 5V readback for 0-5kV output on front panel.

The prototype power supply has been developed and tested successfully. A programme has been taken to fabricate 35 nos. for INGA project.

2.4.10 Development of 1kV/10mA BGO Detector Bias supply for INGA

Rajesh Kumar, S.K. Suman and A. Mandal

A high precision 1kV power supply has been designed to bias BGO Detector to be used in INGA project. About 30 BGO Detectors will be used. A crate based modular design has been adopted, where 10 number of power supplies will be housed in a single 19" custom made crate and powered by a common power source housed in the crate.

It is a voltage regulated 1kV power supply. The heart of the power supply is a high precision linear DC amplifier. The power supply provides an extremely stable, high voltage that is required for proper bias of photo multiplier tubes.

Specifications:

- Bias voltage range : 0-1kV
- Rated output current : 10mA
- Load regulation (20%) : ±0.01%
- Resettability : ±0.1%
- Output ripple : <10mVpp

Features:

- Front panel LCD meter for output voltage/current monitoring
- Output always starts from zero
- Programmable output ramping rate
- Ready signal to indicate stable output
- Safety provided during power fail. Reset provision to restart after power failure.

The prototype has been developed and tested and planned to fabricate 30 nos.

2.4.11 Development of Current Regulated Resonator Heater Power Supply (0 to 10 Watt)

Rajesh Kumar, S.K. Suman, Soumen Kar and A. Mandal

This supply delivers 10W power to a 10Ω heater mounted on a LINAC cavity to have a balance load on refrigerator. When a part of cavities are not working, this power supplies can provide equivalent dynamic load to refrigerator.

This is a 0-1A linearly variable current regulated power supply used to deliver 10Ω power to a 10R heater mounted on resonator in LINAC to balance the heat load. It is crate based modular design, where 10 power supplies will be housed in 19" custom made crate and powered by a common power source.

Specifications:

- Output Current : 0 - 1A
- Output Voltage Range : 12V
- Output Stability : 0.01%

Features:

- LCD display for output power.
- 10 Turn Front Panel Pot for output setting.
- Remote ON/OFF control and readback.
- Output off if load is disconnected.

One such power supply has been fabricated and tested. 30 nos of such power supplies will be fabricated in the next year.

2.4.12 Development of Thyristor (SCR) based single phase AC regulator

Rajesh Kumar, S.K. Suman and A. Mandal

A thyristor based AC regulator has been developed to get the variable AC form the fixed mains AC source. At present we have been using the auto-transformer in high current power supply for regulating AC voltage. Now we are planning to develop thyristor (SCR) technology for development of high current power supply because of high efficiency, compact size and flexibility in control. They are also suitable for close loop operation because of low control power and fast response.

This year we have developed and tested a gate firing circuit of SCR for single phase full wave AC regulator. Test results are :

- Gate firing angle : 180° - 0°
- AC regulation : 0% - 100%

2.4.13 Sixteen bit Input Gate Output Register (IGOR) fabrication

S.K. Suman, Rajesh Kumar and A. Mandal

This is a single width CAMAC module to control the magnet power supplies through CAMAC. Last year 10 nos. of IGOR modules were fabricated and tested for PH-II magnet power supplies.

Features:

- 16-bit Input gate and 16-bit output register with handshaking.
- Two control pulses and one status bit.
- HTL input/output signal.

2.4.14 Development of 2-channel Isolation Amplifier module

S.K. Suman, Rajesh Kumar, A. Mandal

A 2-channel Isolation amplifier module has been developed to make complete isolation for analog control/ read signal between the power supply and CAMAC based controller. This is a single board module which has the following features and applications.

Features:

- Three port isolation : Input, Output and power.
- Wide bandwidth : 20 kHz.
- Rating of analog signal for isolation : ±10V
- Non-linearity : ±0.02% max.

Applications:

- Useful for ground isolation between SMPS power supply and CAMAC module.
- Useful for process signal isolation in data acquisition.

2.5 LOW ENERGY ION BEAM FACILITY

G. Rodrigues, P. Kumar, U.K. Rao, Y. Mathur, S. Kumar, P.S. Lakshmi, C.P. Safvan, D. Kanjilal and A. Roy

A. NANOGAN source operation and maintenance

In the last year, an appreciable amount of time has been devoted to the development of metal ion production. The source has been working satisfactorily with reasonable amount of currents required for experiments related to materials sciences, atomic and molecular physics. However, from source development point of view, the beam currents are limited due to transmission problems from the extraction system and through the beam-line. Strong electric stresses have been observed in the puller region with eventually the puller electrode being displaced off-axes. It has been observed that the beam losses are huge in the extraction region in addition to this effect. The improvement is constantly being worked upon.

For ease of tuning various beams in terms of stability monitoring from the source side and to study the behavior of the plasma under different conditions of source tuning, a resistance network compatible to the beam currents measured was designed and implemented to monitor the output voltage instead of the beam current and simultaneously to look at the behavior on a scope. In a typical tuning of argon beam, a snapshot of the source fluctuations is shown in figure 1. For example, if the fluctuations are too large, it implies that the source is not in a stable condition. Therefore, some of known parameters can be tuned to bring the source in a more stable condition in terms of minimizing the

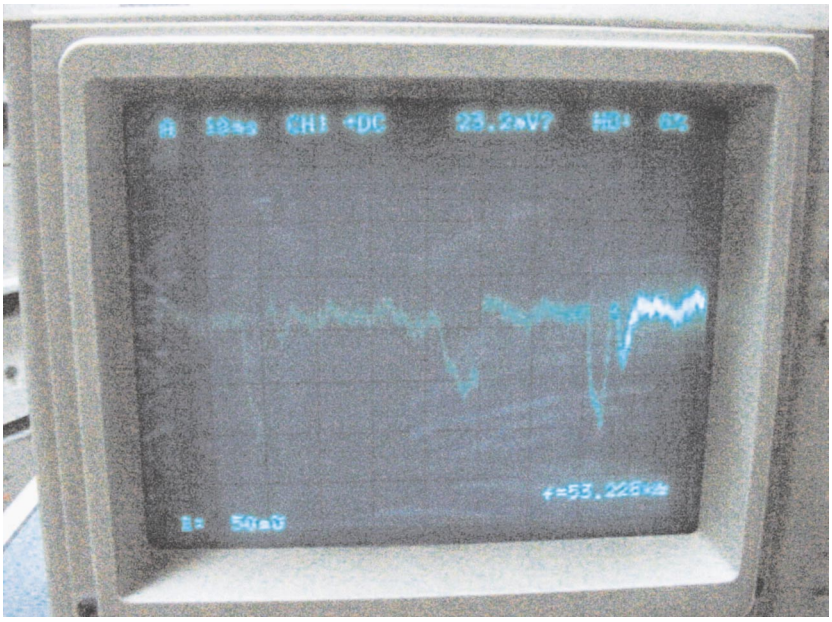

Fig. 1 : Source fluctuations during tuning with Argon beam

fluctuations from the source. In the case of measuring the total integrated beam current, the instantaneous source behavior is not clear and causes confusion.

We have had problems with the 300 kV high voltage deck power supply in terms of severe sparking and burning in one of the high voltage stacks possibly due to one or more of the following reasons. The small gap maintained between the high voltage and ground points and in addition to some of the foreign particles sitting there may be the reasons for this behavior. The 'burnt-out' stack shows that the effect has been taking place over quite a long, extended period of time. A view of the damaged stack is shown in figure 2a. Since the damage was not too severe to the circuit boards, a small board was fabricated and integrated into the stack. The rectified board integrated with the stack is shown in figure 2b. The power supply has been working as per expectations until now.

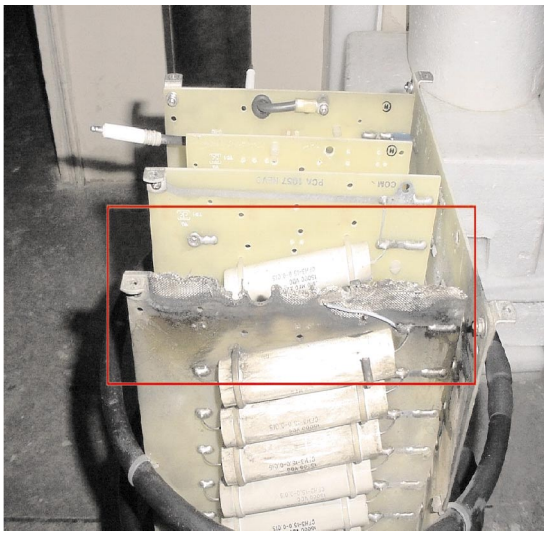

2 (a)

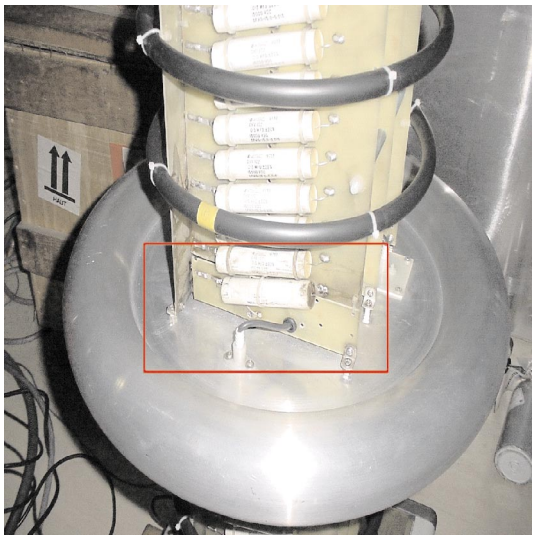

2 (b)

Fig. 2 : (a) Damaged high voltage stack (in red), (b) after rectification (in red)

During operations with the micro-oven system (shown in figure 3.) for generating metal ions, it was found many a time that the oven power supply had malfunctioned. We found that due to the use of metallic elements for generating metal ions, short-circuiting invariably occurred to the oven body and thereby damaging the power supply which inherently had no protection. After some discussions with Pantechnik, France, it became clear that similar problems were being faced by them and therefore it needed a long term solution. Therefore, a new oven power supply with adequate protection but similar ratings was looked into. A Xantrex type oven power supply with short-circuit protection is presently under installation and integration into the 30 kV deck.

For some of the beams like copper where we could not generate sufficient vapour pressure by using the MIVOC method, we instead tried to place the material inside and close to the ECR resonance zone. We found that the method worked very well

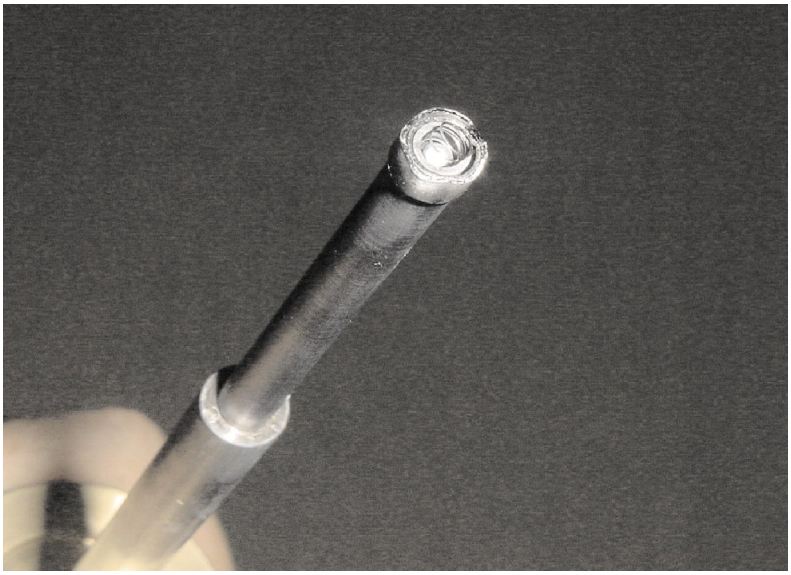

Fig. 3 : View of the micro-oven after a typical beam run

except that the chamber was contaminated and needed to be thoroughly cleaned before the start of the next new beam. Figure 4. shows a typical charge state distribution optimised on Cu^{10+} with argon as a support gas at relatively higher levels of RF power.

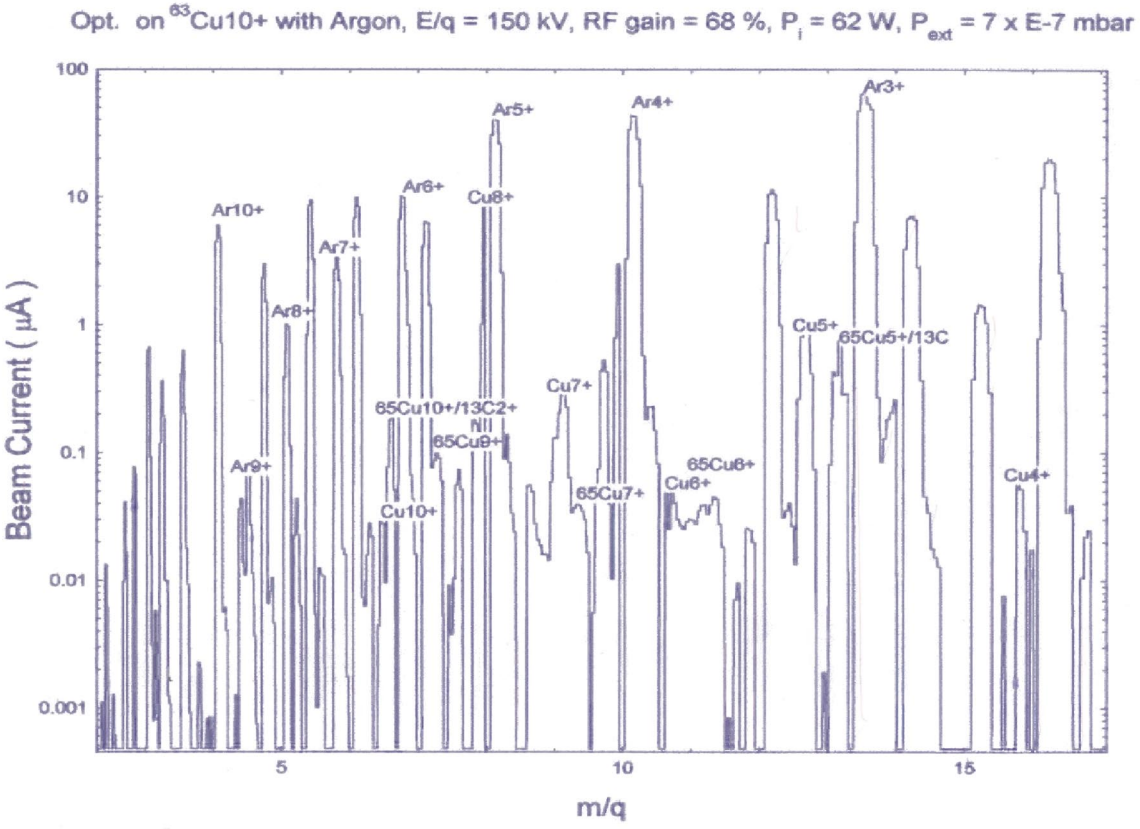

Fig 4. Charge state distribution optimised on Cu^{10+}

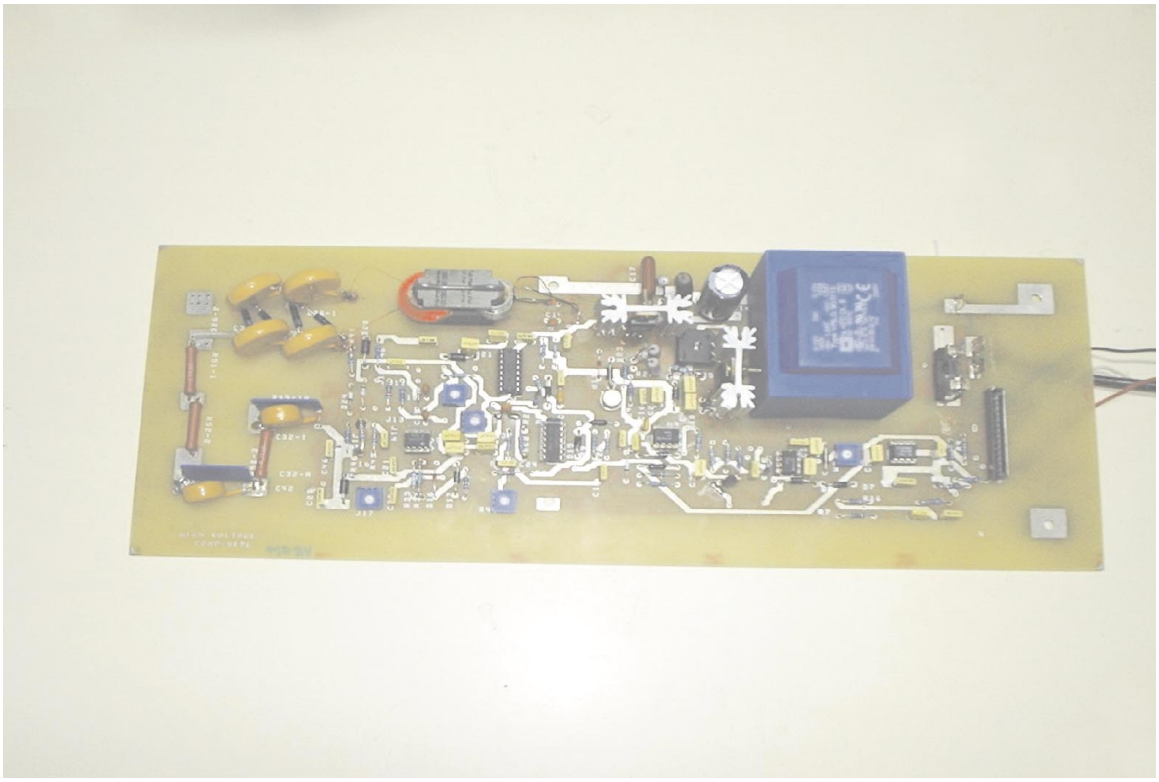

Fig. 5 : Indigenously developed 10 kV, 1 mA high voltage power supply

As part of developmental activity, a high voltage 10 kV, 1 mA power supply was designed, fabricated and tested. After a continuous run for 24 hours, the long term stability was measured to be 0.06 % per 8 hours after a warm-up time of about half hour. The ripple was measured approximately to be 0.06 % rms of the rated voltage at 1 mA load. It is found to decrease linearly to approximately 0.01 % without load.

The Low Energy Ion Beam Facility has been running smoothly during the last year almost full time. Table 1. below lists various experiments performed using this facility.

Table 1. List of experiments performed by various users

	Experiment/Institution	**Beam species**	**Energy**	**Dose**
1.	Formation of ZnO nanoparticles in quartz matrix/Allahabad Univ.	Zn^+,O^+	150 keV, 40 keV	2.5 x 10^{16}, 2 x 10^{17}
2.	Synthesis of SiC in Si matrix/NSC	C^+	110 keV, 150 keV	5 x 10^{17}, 1 x 10^{18}
3.	Formation of SOI layers at elevated temperatures (300^{o}C)/ IOP, Bhubaneswar	N^+	100 keV	5 x 10^{17}

	Experiment/Institution	Beam species	Energy	Dose
4.	Irradiation of Au-Ge thin films to achieve room temperature mixing across interface/ IOP, Bhubaneswar	Ar^{2+},Ar^{4+}	200 keV, 400 keV	5×10^{15}, 1×10^{16}
5.	Irradiation of Au,Ag & Pt thin films for sputtering study/ IOP, Bhubaneswar	Au^{4+}	550 keV,700 keV, 750 keV	1×10^{14} to 1×10^{15}
6.	Study of electrical, structural, thermal and magnetic properties of Al_2O_3, CuO and SiO_2/Univ. of Madras	Fe^{+}	150 keV	5×10^{15}, 5×10^{16}, 5×10^{17}
7.	Study of potential sputtering/ Allahabad Univ.	$Xe^{6+,11+,12+}$	180 keV, 900 keV	1×10^{14},1×10^{15}, 3×10^{15}, 1×10^{16}
8.	Study of optical properties of Ge nanoparticle embedded in SiO_2/IIT, Kharagpur	Ge^{+}	150 keV	3×10^{16}, 1×10^{17}
9.	Synthesis of GaN and study of phase formation (at 400ºC)/ Allahabad Univ	N^{+}	75 keV	4×10^{17}
10.	Synthesis of metal nanoparticles in polymers and study of optical properties/Univ. of Pune	Cu^{3+}	150 keV	1×10^{15}, 1×10^{16}
11.	Study of Cu implanted SiO_2 films/Univ. of Pune	Cu^{2+}	100 keV	5×10^{14}, 3×10^{16}
12.	Formation of ZnO nanostructures/ Allahabad Univ.	Ar^{+}	15 keV	5×10^{15}
13.	Probing of interaction of low energy HCI with liquid droplets/ Univ. of Mysore	Ar^{q+}, N^{q+}	150 keV	-
14.	Implantation on SiO_2 films/NSC	Xe^{2+}	250 keV	5×10^{16}
15.	Study of effect of irradiation on Au/n-Si Schottky diode/NSC	Ar^{7+}	1 MeV	5×10^{13}
16.	Surface topography of damage caused by potential energy of ions/Univ. of Mumbai	$Ar^{2+,6+,9+}$	200 keV	6×10^{11}, to 1×10^{14}

2.6 INSTALLATION OF THE FIRST HIGH TEMPERATURE SUPERCONDUCTING (HTS) ELECTRON CYCLOTRON RESONANCE (ECR) ION SOURCE CALLED PKDELIS AND DEVELOPMENT OF RFQ

G. Rodrigues, P. Kumar, C.P. Safvan, S. Kumar, P.S. Lakshmi, U.K. Rao, Y. Mathur, D. Kanjilal and A. Roy

Fig. 1 : HTS ECR ion source with the extraction system (extreme left).

The world's first High Temperature Superconducting ECR Ion Source is presently under installation. A view of the HTS ECR ion source and related components installed, with the Bi-2223 HTS coils housed in seperate cryostats is shown in figure 1. The HTS coils are cooled to below 23 K for optimum operation. The source is powered by a 18 GHz, 1.5 kW (max) RF generator for igniting the plasma. The plasma chamber is water cooled using a dedicated water cooling system. If the temperature or the water flow rate does not conform to within specified limits, the RF generator will be forced to shut down to protect the plasma chamber and the permanent magnets of the hexapole. A 3-phase 50 kVA uninterruptible power supply (UPS) has been installed for powering all the source related components for continuous operation and smooth running of the system. A separate earth grounding pit has been allocated for the source for safety measures. The source will deliver beams of highly charged ions for various experiments related to atomic and molecular physics at typical extraction voltages ranging from 20 to 30 kV. However, from optics considerations, relatively higher extraction voltages (~ 60 kV) would be necessary in order to reduce the effect of space charge beam blow-up. A medium resolution, large acceptance, air-cooled, analysing magnet has been installed and will transport the ions of interest to the experimental chamber. The test results of the magnet have been satisfactory. The first ignition of the plasma at low RF power levels was successfully accomplished on 14th October 2004 with all related components working satisfactorily. A view of the

first plasma from the injection side is shown in figure 2. The radiation levels around the source were measured at different coil currents in the HTS coils and various RF power levels. At relatively higher coil currents and RF power levels of order of 500 W or so, the radiation levels were maximum at the extraction side of the source and measured to be of the order of 7 rad/hour. In order to be in the safe working limit, lead shielding structures around the source area are necessary. Some of the diagnostics are being set-up to give detailed information of the plasma processes taking place inside the source. Space charge compensation studies would lead to better understanding of beam transport from the source. A Langmuir probe has been designed and will be installed close to the ECR plasma zone to give information on the plasma density. Present status is that all components associated to the source have been thoroughly tested. For example, after a typical cool-down time of about 10 hours or so, the cold heads, cold formers and warm leads are maintained at temperatures of 21 K, 22 K and 208 K respectively.

Due to the different focussing properties of various charge states under the influence of an axial magnetic field, a new extraction system with possibilities of movement of the electrodes for ease of beam tuning is being designed for compatibility with the source. The electrodes will be air/water cooled due to the large beam power of the order of 600 W for the particular case when the source is operated at 60 kV with a total current of 10 mA. The extraction optics have been worked out assuming an electron temperature of 5.0 eV and ion temperature of 0.0 eV with a total source current of 10 mA including the space charge effect.

The trajectories of the ion beam from the ECR plasma are shown in figure 3. Figure 4 shows the geometrical emitances as a function of the geometry of the extraction electrode,

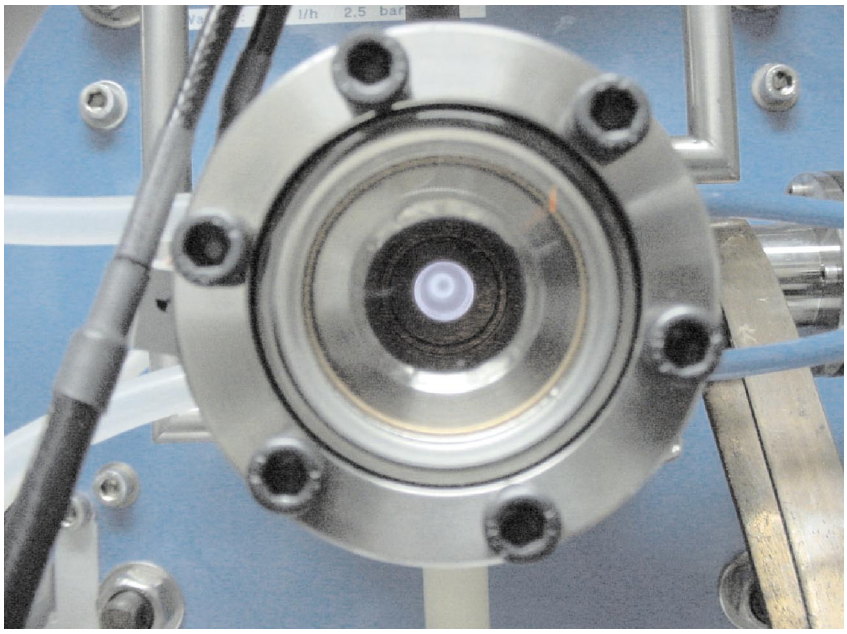

Fig. 2 : View of the ‘first plasma’ from the injection side

puller electrode and the magnetic field. All other related components required for the beam line are ready for integration into the system. Figure 5 shows the possible beams deliverable from the PKDELIS source for injection into the LINAC.

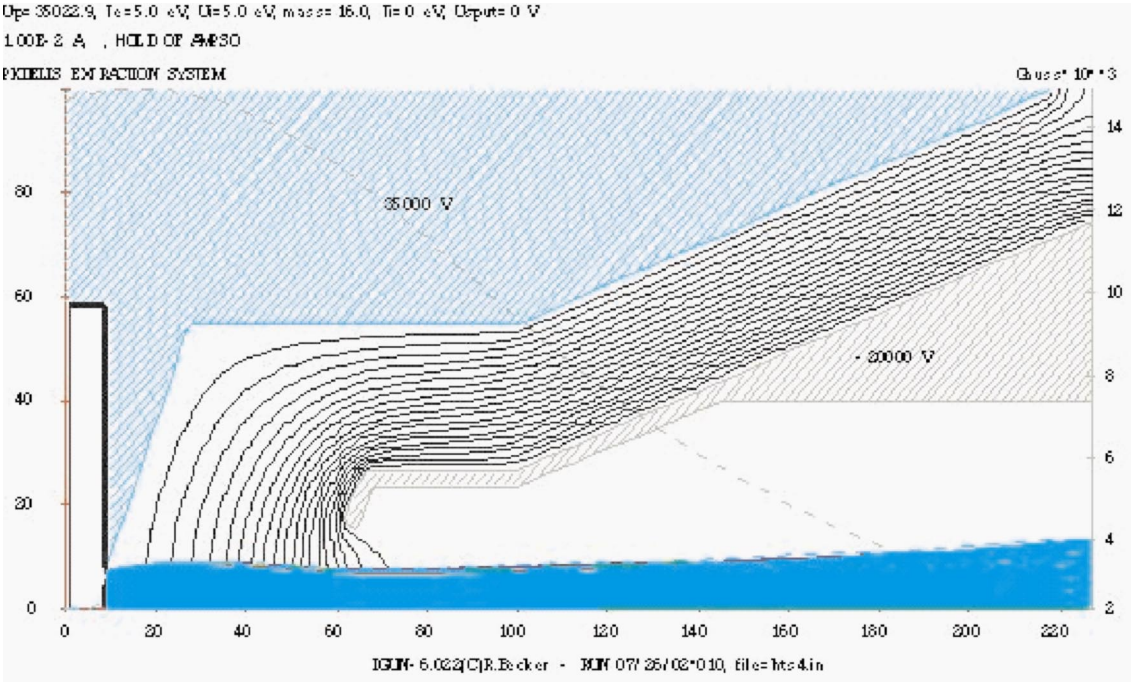

Fig. 3 : Trajectories of the ion beam from ECR plasma

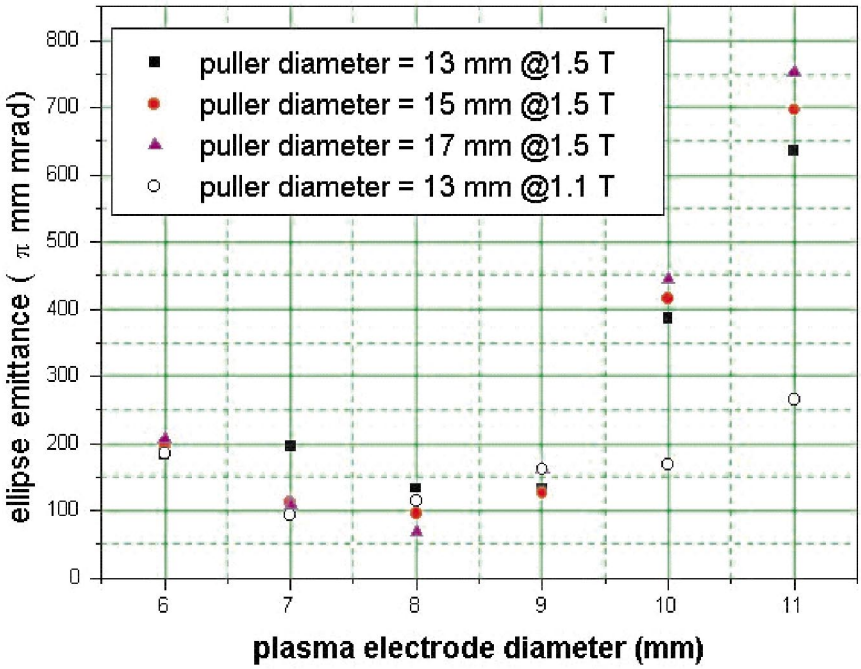

Fig. 4 : Beam emittance from PKDELIS source

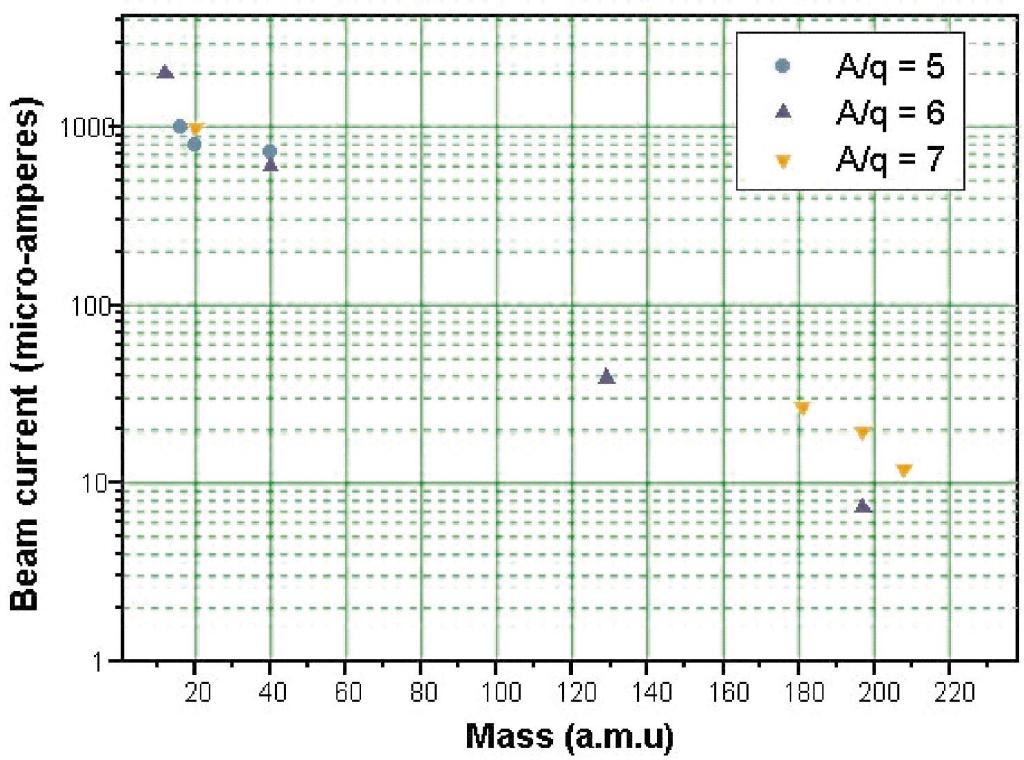

Fig. 5 : Beams deliverable from the PKDELIS source for transport through LINAC

To accelerate the ions from the ECR ion source a room temperature Radio Frequency Quadrupole accelerator is being designed and fabricated. The accelerator is being designed to accept particles of mass by charge ratio of 7 at 8 keV/u. The RFQ will accelerate and bunch these beams to 300keV/u which will be further accelerated by a drift tube LINAC (or low beta cavity) structure. The RFQ will operate at 48.5 MHz (to match with the existing 97 MHz superconducting LINAC structure).

Radio Frequency cavity structure simulations have been carried out to design an easily machinable cavity that resonates at 48.5 MHz, keeping nearby RF mode spacings as far as possible. Reducing the physical dimensions to practical values is also an important consideration. The final structure is a combination of the features of already existing RFQ accelerators, most notably the CERN REX-ISOLDE and the RIKEN RFQ's.

Beam optics simulations to determine the detailed vane structure of the RFQ accelerator, and to investigate the beam dynamics (energetics and emittance growth, tolerance to beam misalignments) are being carried out using standard software like LIDOS as also in house developed code.

A prototype RFQ to test these simulations is under construction to measure the RF properties like resonant frequency, tunability, Q values, field uniformity and mechanical

properties like stability and water cooling systems. The design concept of the RFQ vane holding systems is shown in the attached figure (the cavity is not shown).

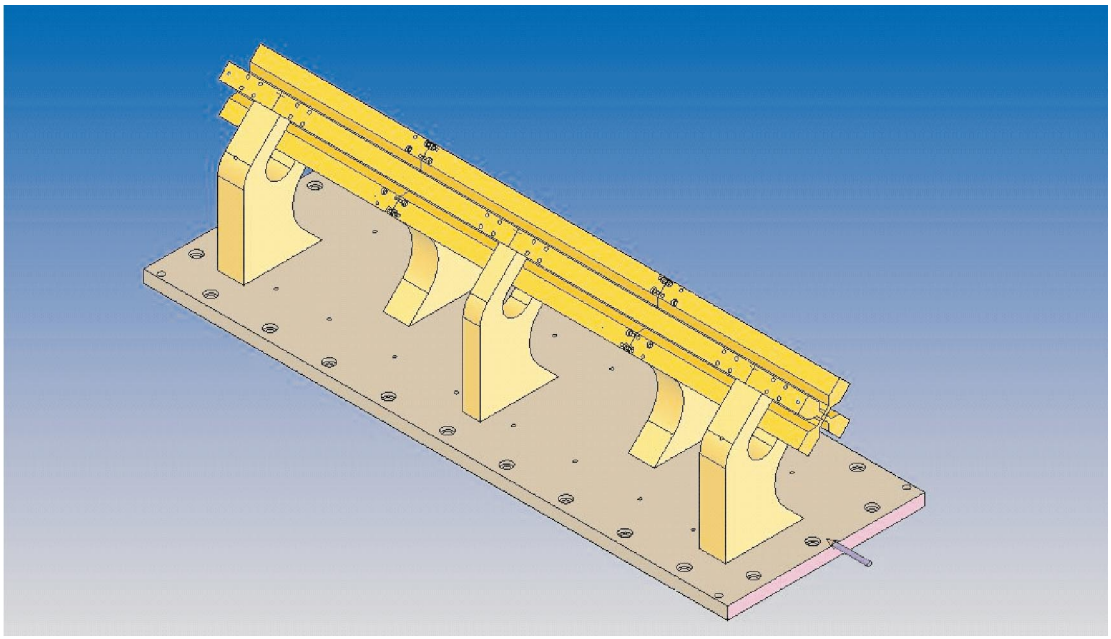

Fig. 6 : Development of Radio frequency quadrupole accelerator